

Detecting the polarization in $\chi_{cJ} \rightarrow \phi\phi$ decays to probe hadronic loop effect

Qi Huang^{1,*}, Jun-Zhang Wang^{2,3,†}, Rong-Gang Ping^{1,4,‡} and Xiang Liu^{2,3,5,§}

¹University of Chinese Academy of Sciences (UCAS), Beijing 100049, China

²School of Physical Science and Technology, Lanzhou University, Lanzhou 730000, China

³Research Center for Hadron and CSR Physics, Lanzhou University and Institute of Modern Physics of CAS, Lanzhou 730000, China

⁴Institute of High Energy Physics, Chinese Academy of Sciences, P.O. Box 918(1), Beijing 100049, China

⁵Lanzhou Center for Theoretical Physics, Key Laboratory of Theoretical Physics of Gansu Province, and Frontier Science Center for Rare Isotopes, Lanzhou University, Lanzhou 730000, China

In this work, we propose that detecting the polarization information of $\chi_{cJ} \rightarrow \phi\phi$ ($J = 0, 1, 2$) can be as good test of the role of hadronic loop effect on these decays. Our results shows that the obtained ratios of helicity amplitudes are quite stable, which are $|F_{1,1}^{(0)}/F_{0,0}^{(0)}| \approx 0.359$, $|F_{1,0}^{(1)}/F_{0,1}^{(1)}| = 1$, $|F_{1,1}^{(1)}/F_{0,1}^{(1)}| = 0$, $|F_{1,0}^{(2)}/F_{0,0}^{(2)}| = |F_{0,1}^{(2)}/F_{0,0}^{(2)}| \approx 1.285$, $|F_{1,-1}^{(2)}/F_{0,0}^{(2)}| = |F_{-1,1}^{(2)}/F_{0,0}^{(2)}| \approx 5.110$ and $|F_{-1,-1}^{(2)}/F_{0,0}^{(2)}| = |F_{1,1}^{(2)}/F_{0,0}^{(2)}| \approx 0.465$. By adopting these predicted ratios, we further generate Monte-Carlo events of moments $\langle t_{ij} \rangle$, which are directly related to the determination of helicity amplitudes. We suggest further experiments like BESIII and Belle II to perform an analysis on the polarizations of the $\chi_{cJ} \rightarrow \phi\phi$ process in the future, which is important to understand the underlying decay mechanism existing in χ_{cJ} decays.

I. INTRODUCTION

How to quantitatively depict non-perturbative behavior of strong interaction is full of challenge and opportunity. In the past two decades, more and more novel phenomena involved in hadron spectroscopy were observed with the accumulation of experimental data, which provide an ideal platform to understand non-perturbative behavior of strong interaction.

Among these reported novel phenomena, the anomalous decay behavior of χ_{cJ} decays into two light vector mesons [1, 2] has attracted theorist's attention to decode the underlying mechanism for governing these decays, where the hadronic loop mechanism [3–24] was introduced and found to be important when reproducing the measured branching ratios [6, 7].

In fact, the information of branching ratios is not whole aspect involved in the χ_{cJ} decays into two light vector mesons. Obviously, finding out other crucial evidence of hadronic loop effect on the χ_{cJ} decays into two light vector mesons is an interesting research issue.

In this work, with the $\chi_{cJ} \rightarrow \phi\phi$ ($J = 0, 1, 2$) decays as example, we show that detecting the polarization information of $\chi_{cJ} \rightarrow \phi\phi$ can be as an effective way to probe hadronic loop mechanism. In the present work, we present a concrete polarization analysis on $\chi_{cJ} \rightarrow \phi\phi$ associated with a calculation of the $\chi_{cJ} \rightarrow \phi\phi$ decays when considering hadronic loop mechanism. We find that the obtained ratios of helicity amplitudes are quite stable, by which a further Monte-Carlo (MC) events of moments $\langle t_{ij} \rangle$ are also generated. By this investigation, we strongly suggest that BESIII and Belle II should pay more attentions to the measurement of polarization information of $\chi_{cJ} \rightarrow \phi\phi$, which may provide crucial test to the hadronic loop mechanism.

This paper is organized as follows. After the introduction, we give a polarization analysis of the process $\chi_{cJ} \rightarrow \phi\phi \rightarrow 2(K^+K^-)$ in Sec. II. And then, the detailed calculation of $\chi_{cJ} \rightarrow \phi\phi$ via charmed meson loop is presented in Sec. III. After that, the numerical results are given in Sec. IV. Finally, this paper ends with a summary.

II. POLARIZATION ANALYSIS

We analyze the $\phi\phi$ polarization with the motivation to reveal the χ_{cJ} decay mechanism. In the unpolarized e^+e^- collider, the production of $\psi(2S)$ particle is tensor polarized, without longitudinal polarization [25]. The subsequent $\psi(2S) \rightarrow \gamma\chi_{cJ}$ decay may transfer some polarization to the χ_{cJ} states, which is manifested in the $\chi_{cJ} \rightarrow \phi\phi$ decay, showing up the unflat angular distribution of the decayed ϕ meson.

The spin density matrix (SDM) for the $\phi\phi$ system encodes the full polarization information, transferred from the χ_{cJ} decays. In experiment, the measurement on the $\phi\phi$ SDM plays the role to study the χ_{cJ} decay mechanism, given that the polarization patten is predicted based on the decay-dynamical models. We follow the standard way to construct the SDM for the identical particle $\phi\phi$ system.

For a spin- s particle, its spin density matrix is given in terms of multipole parameters, $r_{M,s}^L$, as [26]

$$\rho = \frac{1}{2s+1} \left(\mathcal{I} + 2s \sum_{L=1}^{2s} \sum_{M=-L}^L r_{M,s}^L Q[s, L, M] \right), \quad (1)$$

where \mathcal{I} denotes a $(2s+1) \times (2s+1)$ dimensional unit matrix. The SDM for $\phi\phi$ system can be constructed from the ϕ individual ones, and an easy way is to decompose it into Q matrices multiplied by a set of real parameters, which reads

*Electronic address: huangqi@ucas.ac.cn

†Electronic address: wangjzh2012@lzu.edu.cn

‡Electronic address: pingrg@ihep.ac.cn

§Electronic address: xiangliu@lzu.edu.cn

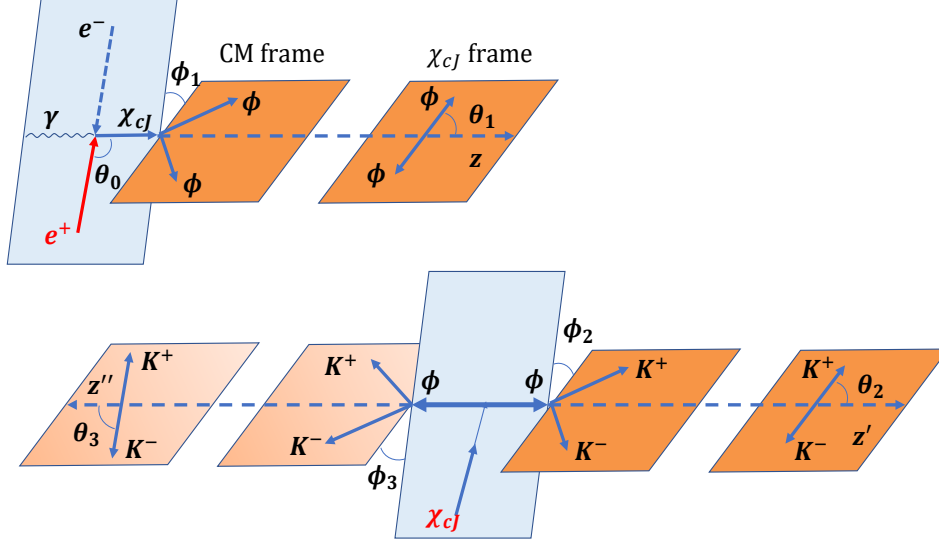


FIG. 1: Helicity system and angles definition for the $\psi(2S) \rightarrow \gamma \chi_{cJ}, \chi_{cJ} \rightarrow \phi\phi, \phi \rightarrow K^+K^-$ process.

as

$$\begin{aligned} \rho_{\phi\phi} &= \rho_{\phi} \otimes \rho_{\phi} \\ &= \frac{1}{9} \left[C_{00} \mathcal{I}_3 \otimes \mathcal{I}_3 + 2 \sum_{i=1}^8 (C_{i0} Q_i \otimes \mathcal{I}_3 \right. \\ &\quad \left. + C_{0i} \mathcal{I}_3 \otimes Q_i) + 4 \sum_{i,j=1}^8 C_{ij} Q_i \otimes Q_j \right]. \end{aligned} \quad (2)$$

Here, \mathcal{I}_3 denotes a 3×3 identity matrix. And, the real parameters C_{ij} is determined from the $\phi\phi$ production process, which carry polarization information for the two ϕ mesons. C_{i0} or C_{0i} means that the polarization is detected only for one ϕ meson, while C_{ij} measures the polarization correlation between two $\phi\phi$ mesons. And then, $Q_1 = Q[1, 1, -1]$, $Q_2 = Q[1, 1, 0]$, $Q_3 = Q[1, 1, 1]$, $Q_4 = Q[1, 2, -2]$, $Q_5 = Q[1, 2, -1]$, $Q_6 = Q[1, 2, 0]$, $Q_7 = Q[1, 2, 1]$, $Q_8 = Q[1, 2, 2]$.

The polarization of $\phi\phi$ system is inaccessible in a general purpose of electromagnetic spectrometer at the modern e^+e^- colliders. Nonetheless, the subsequential decay, $\phi \rightarrow K^+K^-$, can be used as the polarimeter to measure the ϕ polarization by studying the implications of the decayed Kaon angular distribution.

We formulate the $\phi\phi \rightarrow 2(K^+K^-)$ decays with helicity amplitude method, which is defined in the helicity system as shown in Fig. 1. One ϕ decaying into K^+K^- pair is described with helicity angles (θ_2, ϕ_2) , where θ_2 is the angle spanned between the directions of K^+ and the ϕ momenta, which are defined in the rest frames of their respective mother particles. The azimuthal angle ϕ_2 is defined as the angle between the $\phi\phi$ production plane and the ϕ decay plane. The helicity angles, (θ_3, ϕ_3) , describing another ϕ meson decay, is defined by following the same rule (see Table I). Then the joint angular distribution for $\phi\phi \rightarrow 2(K^+K^-)$ reads as

TABLE I: Definitions of helicity angles and amplitudes in the $\chi_{cJ} \rightarrow \phi\phi$, and $\phi\phi \rightarrow 2(K^+K^-)$ decays.

Decay	Angles	Amplitude
$\chi_{cJ} \rightarrow \phi(\lambda_1)\phi(\lambda_2)$	(θ_1, ϕ_1)	$F_{\lambda_1, \lambda_2}^{(J)}$
$\phi(\lambda_1) \rightarrow K^+K^-$	(θ_2, ϕ_2)	f
$\phi(\lambda_2) \rightarrow K^+K^-$	(θ_3, ϕ_3)	f

$$|\mathcal{M}|^2 \propto \text{Tr}[\rho_{\phi\phi} \cdot M_a \otimes M_b^\dagger]$$

$$= t_{00} C_{00} + \sum_{i=1}^8 (t_{i0} C_{i0} + t_{0i} C_{0i}) + \sum_{i,j=1}^8 t_{ij} C_{ij} \quad (3)$$

with

$$(M_a)_{\lambda_1, \lambda'_1} = D_{\lambda_1, 0}^{1*}(\phi_2, \theta_2, 0) D_{\lambda'_1, 0}^1(\phi_2, \theta_2, 0) f^2, \quad (4)$$

$$(M_b)_{\lambda_2, \lambda'_2} = D_{\lambda_2, 0}^{1*}(\phi_3, \theta_3, 0) D_{\lambda'_2, 0}^1(\phi_3, \theta_3, 0) f^2. \quad (5)$$

For simplicity, we take $f^2 = 1$. The joint angular distribution can be further decomposed into the $\phi\phi$ polarization in terms of the real multipole parameters C_{ij} . The t_{ij} factors play the role of the spin observables corresponding to the parameters C_{ij} . The term t_{00} is the unpolarization cross section, while $t_{0L}(t_{L0})$ corresponds to the observable for detecting one ϕ polarization with rank L , and leaving another ϕ polarization being undetected. The term t_{ij} denotes the spin correlation between the two ϕ 's. Expressions of t_{ij} factors are given in terms of angles θ_i and ϕ_i ($i = 2, 3$) as shown in Appendix A.

The multipole parameters, C_{ij} , in the $\rho_{\phi\phi}$ SDM contain the dynamical information of the $\chi_{cJ} \rightarrow \phi\phi$ decays, which can be related to the decay helicity amplitudes $F_{\lambda_1, \lambda_2}^{(J)}$. Thus, any theoretical prediction on their values can be tested by measuring their spin observables in experiment.

We relate the parameter C_{ij} to the helicity amplitude $F_{\lambda_1, \lambda_2}^{(J)}$ by calculating the spin density matrix $\rho_{\phi\phi}$ of the decay $\chi_{cJ} \rightarrow \phi\phi$, which reads as

$$\rho_{\phi\phi} = N \cdot \rho_J \cdot N^\dagger, \quad (6)$$

where ρ_J is a spin density matrix for χ_{cJ} with $J = 0, 1, 2$ for χ_{c0}, χ_{c1} and χ_{c2} , respectively. N denotes decay matrix, which can be written as

$$(N)_{\lambda_1 \lambda_2 \lambda'_1 \lambda'_2, M} = D_{M, \lambda_1 - \lambda_2}^{J*}(\phi_1, \theta_1, 0) \times D_{M, \lambda'_1 - \lambda'_2}^J(\phi_1, \theta_1, 0) F_{\lambda_1, \lambda_2}^{(J)*} F_{\lambda'_1, \lambda'_2}^{(J)}, \quad (7)$$

where (θ_1, ϕ_1) are the helicity angles describing the ϕ meson flying direction as shown in Fig. 1. Azimuthal ϕ_1 is defined as the angle between the ϕ production and decay planes, while θ_1 is the angle spanned between the ϕ and χ_{cJ} momenta. $F_{\lambda_1, \lambda_2}^{(J)}$ denotes the helicity amplitude in terms of two ϕ helicity values λ_1 and λ_2 .

A special decay is $\chi_{c0} \rightarrow \phi\phi$, where the χ_{c0} spin density is reduced to Kronecker delta function, *i.e.*, $\rho_0 = \delta_{\lambda_1, \lambda_2} \delta_{\lambda'_1, \lambda'_2}$. Then the multipole parameters C_{ij} are calculated to be

$$C_{00} = 9 |F_{0,0}^{(0)}|^2 + 18 |F_{1,1}^{(0)}|^2, \quad (8)$$

$$C_{44} = -\frac{3}{2} |F_{1,1}^{(0)}|^2, \quad (9)$$

$$C_{55} = -C_{77} = -\frac{3}{4} (F_{1,1}^{(0)*} F_{0,0}^{(0)} + F_{0,0}^{(0)*} F_{1,1}^{(0)}), \quad (10)$$

$$C_{60} = C_{06} = |F_{1,1}^{(0)}|^2 - |F_{0,0}^{(0)}|^2, \quad (11)$$

$$C_{66} = |F_{0,0}^{(0)}|^2 + \frac{|F_{1,1}^{(0)}|^2}{2}, \quad (12)$$

$$C_{88} = \frac{3 |F_{1,1}^{(0)}|^2}{2}, \quad (13)$$

while other $C_{i,j}$ parameters are vanishing due to the spin-parity conservation in the $\chi_{c0} \rightarrow \phi\phi$ decays.

Then, with the helicity amplitude $F_{\lambda_1, \lambda_2}^{(0)}$, the ϕ angular distribution from the $\chi_{c0} \rightarrow \phi\phi$ decay can be expressed as

$$\begin{aligned} \mathcal{W}_0 \propto & \cos(\phi_{23}) [4 \sin^2(\theta_2) \sin^2(\theta_3) \cos(\phi_{23}) |F_{1,1}^{(0)}|^2 \\ & + \sin(2\theta_2) \sin(2\theta_3) 2\text{Re}(F_{1,1}^{(0)*} F_{0,0}^{(0)})] \\ & + 4 \cos^2(\theta_2) \cos^2(\theta_3) |F_{0,0}^{(0)}|^2, \end{aligned} \quad (14)$$

where $\phi_{23} = \phi_2 + \phi_3$.

One can see that the ϕ angular distribution for the $\chi_{c0} \rightarrow \phi\phi$ decay is reduced to a uniform distribution either on the $\cos\theta_2(\cos\theta_3)$ or $\phi_2(\phi_3)$ observables alone. Spin correlation for $\phi\phi$ system can only be observed by measuring a moment formed by the angles θ_i and ϕ_i ($i = 2, 3$) simultaneously.

The strong decay $\chi_{c1} \rightarrow \phi\phi$ conserves the parity. Thus, the helicity amplitudes satisfy the relation $F_{-\lambda_1, -\lambda_2}^{(1)} = -F_{\lambda_1, \lambda_2}^{(1)}$, especially $F_{0,0}^{(1)} = 0$. And then, the amplitudes are reduced to three independent components, *i.e.*, $F_{1,1}^{(1)}, F_{1,0}^{(1)}$ and $F_{0,1}^{(1)}$. The

matrix of amplitudes is taken as

$$(F_{\lambda_1, \lambda_2}^{(1)}) = \begin{pmatrix} F_{1,1}^{(1)} & F_{1,0}^{(1)} & 0 \\ -F_{1,0}^{(1)} & 0 & -F_{0,1}^{(1)} \\ 0 & -F_{1,0}^{(1)} & -F_{1,1}^{(1)} \end{pmatrix}. \quad (15)$$

As for the χ_{c1} production from the decay $\psi(2S) \rightarrow \gamma\chi_{c1}$, its SDM is well defined and taken as $\rho_1 = \frac{1}{4} \text{diag}\{1, 2, 1\}$ [25] in its rest frame. Here, the nonvanishing parameters C_{i0}, C_{0i} and C_{ij} are calculated and given in Appendix B.

The ϕ meson has nonzero decay width, the masses of two $\phi\phi$ may have different values from the χ_{c1} decay in a given event. However, its narrow decay width allows us to treat the $\phi\phi$ as an identical particle system statistically. Then, Exchanging two ϕ mesons yields asymmetry relation $F_{1,0}^{(1)} = -F_{0,1}^{(1)}$, and $F_{1,1}^{(1)} = 0$, where the joint angular distribution is independent on the amplitude, and it reads

$$\mathcal{W}_1 \propto (2 + \sin^2 \theta_1) [\cos^2 \theta_2 \sin^2 \theta_3 + \sin^2 \theta_2 \cos^2 \theta_3]. \quad (16)$$

Similarly, we perform the same analysis of the $\chi_{c2} \rightarrow \phi\phi$ decay, and we take the χ_{c2} SDM as $\rho_2 = \frac{3}{20} \text{diag}\{2, 1, 2/3, 1, 2\}$ [25]. Take into consideration of parity conservation in this decay, one has the relation $F_{-\lambda_1, -\lambda_2}^{(2)} = F_{\lambda_1, \lambda_2}^{(2)}$, then the amplitude matrix is reduced to be

$$(F_{\lambda_1, \lambda_2}^{(2)}) = \begin{pmatrix} F_{1,1}^{(2)} & F_{1,0}^{(2)} & F_{1,-1}^{(2)} \\ F_{0,1}^{(2)} & F_{0,0}^{(2)} & F_{0,-1}^{(2)} \\ F_{1,-1}^{(2)} & F_{1,0}^{(2)} & F_{1,1}^{(2)} \end{pmatrix}. \quad (17)$$

With these considerations, the multipole parameters are calculated and given in Appendix C, and these expressions can be further simplified using the relation $F_{\lambda_1, \lambda_2}^{(2)} = F_{\lambda_2, \lambda_1}^{(2)}$ if one takes the $\phi\phi$ as an identical particle system.

III. MESON LOOP EFFECTS IN $\chi_{cJ} \rightarrow \phi\phi$ DECAY

Under the hadronic loop mechanism, the $\chi_{cJ} \rightarrow \phi\phi$ decays occur via the triangle loops composed of $D_{(s)}^{(*)}$ and $\bar{D}_{(s)}^{(*)}$, where these loops play the role of bridge to connect the initial χ_{cJ} and final states. In Figs. 2-4, we present the Feynman diagrams depicting the $\chi_{cJ} \rightarrow \phi\phi$ transitions.

To calculate the decay amplitudes shown in Fig. 2-4, we adopt the effective Lagrangian approach, thus at first we should introduce the effective Lagrangians relevant to our calculation. For the interaction between χ_{cJ} and a pair of heavy-light mesons, the general form of the effective Lagrangian can be constructed under the chiral and heavy quark limits [27]

$$\mathcal{L}_p = ig_1 \text{Tr} [P^{(Q\bar{Q})\mu} \bar{H}^{(Qq)} \gamma_\mu \bar{H}^{(Q\bar{q})}] + H.c., \quad (18)$$

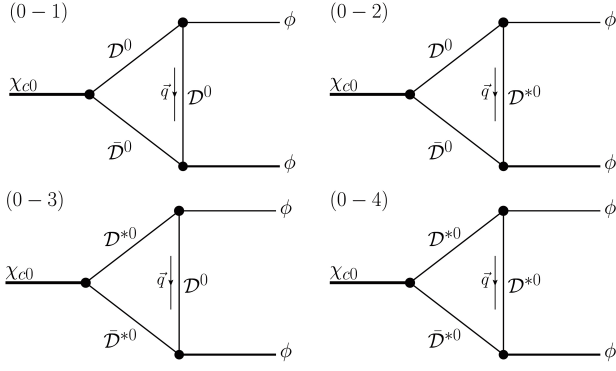


FIG. 2: The Feynman diagrams depicting the $\chi_{c0} \rightarrow \phi\phi$ process via D meson loop.

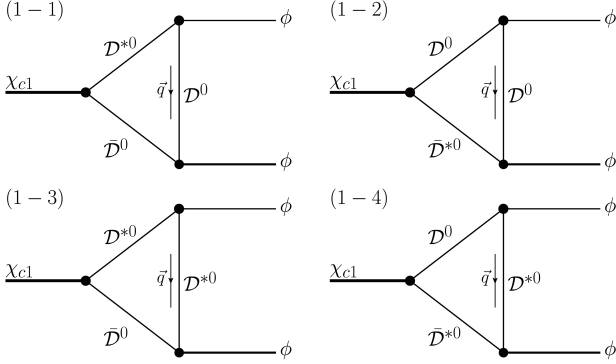


FIG. 3: The Feynman diagrams depicting the $\chi_{c1} \rightarrow \phi\phi$ process via D meson loop.

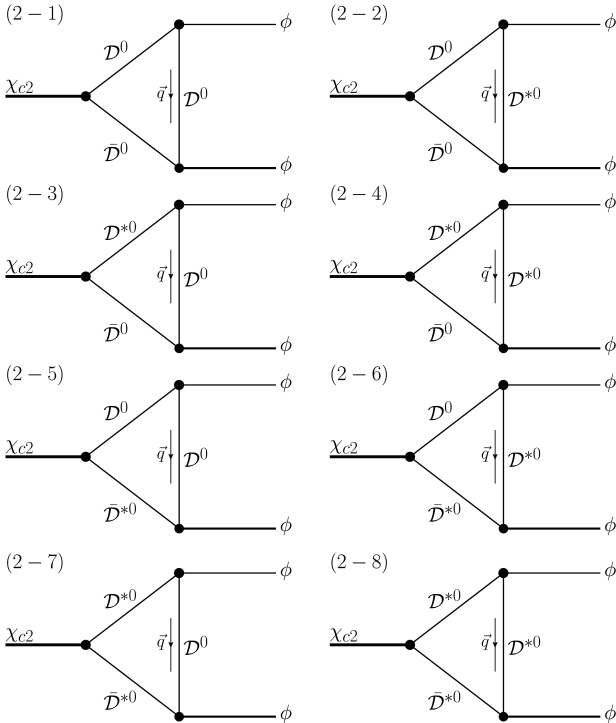


FIG. 4: The Feynman diagrams depicting the $\chi_{c2} \rightarrow \phi\phi$ process via D meson loop.

where $P^{(Q\bar{Q})}$ and $H^{(Q\bar{q})}$ denote the P-wave multiplet of charmonia and $(\mathcal{D}, \mathcal{D}^*)$ doublet, respectively. Their detailed expressions, as shown in Ref. [10, 27–29], can be written as

$$P^{(Q\bar{Q})\mu} = \frac{1+\not{v}}{2} \left[\chi_{c2}^{\mu\alpha} \gamma_\alpha + \frac{1}{\sqrt{2}} \varepsilon^{\mu\alpha\beta\gamma} v_\alpha \gamma_\beta \chi_{c1\gamma} + \frac{1}{\sqrt{3}} (\gamma^\mu - v^\mu) \chi_{c0} + h_c^\mu \gamma_5 \right] \frac{1-\not{v}}{2}, \quad (19)$$

$$H^{(Q\bar{q})} = \frac{1+\not{v}}{2} [\mathcal{D}_\mu^* \gamma^\mu - \mathcal{D} \gamma^5], \quad (20)$$

respectively, with definitions $\mathcal{D}^{(*)\dagger} = (D^{(*)+}, D^{(*)0}, D_s^{(*)0})$ and $\mathcal{D}^{(*)} = (D^{(*)-}, \bar{D}^{(*)0}, \bar{D}_s^{(*)0})^T$. $H^{(Q\bar{q})}$ corresponds to the doublet formed by homologous heavy-light anti-mesons, which can be obtained by applying the charge conjugation operation to $H^{(Q\bar{q})}$.

For the interaction between a light vector meson and two heavy-light mesons, the general form of the Lagrangian reads as [27, 30–34]

$$\mathcal{L}_V = i\beta \text{Tr}[H^j v^\mu (-\rho_\mu)_j^i \bar{H}_i] + i\lambda \text{Tr}[H^j \sigma^{\mu\nu} F_{\mu\nu}(\rho) \bar{H}_i], \quad (21)$$

where

$$\rho_\mu = i \frac{g_V}{\sqrt{2}} \mathcal{V}_\mu, \quad (22)$$

$$F_{\mu\nu}(\rho) = \partial_\mu \rho_\nu - \partial_\nu \rho_\mu + [\rho_\mu, \rho_\nu], \quad (23)$$

and a vector octet \mathcal{V} has the form [7]

$$\mathcal{V} = \begin{pmatrix} \frac{\rho^0}{\sqrt{2}} + \kappa \omega^P + \zeta \phi^P & \rho^+ & K^{*+} \\ \rho^- & -\frac{\rho^0}{\sqrt{2}} + \kappa \omega^P + \zeta \phi^P & K^{*0} \\ K^{*-} & \bar{K}^{*0} & \delta \omega^P + \sigma \phi^P \end{pmatrix}, \quad (24)$$

with

$$\begin{aligned} \kappa &= \frac{\cos \theta}{\sqrt{2}}, & \zeta &= \frac{\sin \theta}{\sqrt{2}}, \\ \delta &= -\sin \theta, & \sigma &= \cos \theta. \end{aligned} \quad (25)$$

By expanding the Lagrangians in Eqs. (18) and (21), we can get the following explicit forms of Lagrangians

$$\begin{aligned} \mathcal{L}_{\chi_{cJ} \mathcal{D}^{(*)} \mathcal{D}^{(*)}} &= -g_{\chi_{c0}} \mathcal{D} \mathcal{D} \chi_{c0} \mathcal{D} \mathcal{D}^\dagger - g_{\chi_{c0}} \mathcal{D}^* \mathcal{D}^* \chi_{c0} \mathcal{D}_\mu^* \mathcal{D}^{*\mu\dagger} \\ &\quad + i g_{\chi_{c1}} \mathcal{D} \mathcal{D}^* \chi_{c1}^\mu (\mathcal{D}_\mu^* \mathcal{D}^\dagger - \mathcal{D} \mathcal{D}_\mu^{*\dagger}) \\ &\quad - g_{\chi_{c2}} \mathcal{D} \mathcal{D} \chi_{c2}^{\mu\nu} \partial_\mu \mathcal{D} \partial_\nu \mathcal{D}^\dagger \\ &\quad + g_{\chi_{c2}} \mathcal{D}^* \mathcal{D}^* \chi_{c2}^{\mu\nu} (\mathcal{D}_\mu^* \mathcal{D}_\nu^{*\dagger} + \mathcal{D}_\nu^* \mathcal{D}_\mu^{*\dagger}) \\ &\quad - i g_{\chi_{c2}} \mathcal{D}^* \mathcal{D} \varepsilon_{\mu\nu\alpha\beta} \partial^\alpha \chi_{c2}^{\mu\rho} (\partial_\rho \mathcal{D}^* \partial^\beta \mathcal{D}^\dagger - \partial^\beta \mathcal{D} \partial_\rho \mathcal{D}^{*\nu\dagger}), \end{aligned} \quad (26)$$

$$\begin{aligned} \mathcal{L}_{\mathcal{D}^{(*)} \mathcal{D}^{(*)} \mathcal{V}} &= -i g_{\mathcal{D} \mathcal{V}} \mathcal{D}_i^\dagger \overset{\leftrightarrow}{\partial}^{\mu} \mathcal{D}^j (\mathcal{V}_\mu)_j^i \\ &\quad - 2 f_{\mathcal{D}^* \mathcal{V}} \varepsilon_{\mu\nu\alpha\beta} (\partial^\mu \mathcal{V}^\nu)_j^i (\mathcal{D}_i^\dagger \overset{\leftrightarrow}{\partial}^{\alpha} \mathcal{D}^{*\beta j} - \mathcal{D}_i^{*\beta\dagger} \overset{\leftrightarrow}{\partial}^{\alpha} \mathcal{D}^j) \\ &\quad + i g_{\mathcal{D}^* \mathcal{V}} \mathcal{D}_i^{*\nu\dagger} \overset{\leftrightarrow}{\partial}^{\mu} \mathcal{D}_\nu^{*j} (\mathcal{V}_\mu)_j^i \\ &\quad + 4 i f_{\mathcal{D}^* \mathcal{V}} \mathcal{D}_{i\mu}^{*\dagger} (\partial^\mu \mathcal{V}^\nu - \partial^\nu \mathcal{V}^\mu)_j^i \mathcal{D}_\nu^{*j}. \end{aligned} \quad (27)$$

With these Lagrangians given in Eq. (26) and Eq. (27), the amplitudes of $\chi_{cJ} \rightarrow \phi\phi$ then can be written out. For $\chi_{c0} \rightarrow \phi\phi$ transition, with $\tilde{g}_{\mu\nu}(p) \equiv -g_{\mu\nu} + \frac{p_\mu p_\nu}{m_p^2}$ the amplitudes corresponding to Fig. 2 are

$$\begin{aligned} \mathcal{M}_{(0-1)} = & \int \frac{d^4 q}{(2\pi)^4} \frac{1}{k_1^2 - m_D^2} \frac{1}{k_2^2 - m_D^2} \frac{1}{q^2 - m_D^2} \mathcal{F}^2(q^2) \\ & \times [-g_{\chi_{c0} \mathcal{D} \mathcal{D}}] [-g_{\mathcal{D} \mathcal{D} \phi} \epsilon_\phi^*(p_2)(k_{1\zeta} + q_\zeta)] \\ & \times [-g_{\mathcal{D} \mathcal{D} \phi} \epsilon_\phi^*(p_3)(q_\lambda - k_{2\lambda})], \end{aligned} \quad (28)$$

$$\begin{aligned} \mathcal{M}_{(0-2)} = & \int \frac{d^4 q}{(2\pi)^4} \frac{1}{k_1^2 - m_D^2} \frac{1}{k_2^2 - m_D^2} \frac{\tilde{g}_{\xi\sigma}(q)}{q^2 - m_{D^*}^2} \mathcal{F}^2(q^2) \\ & \times [-g_{\chi_{c0} \mathcal{D} \mathcal{D}}] [-2f_{\mathcal{D} \mathcal{D}^* \phi} \epsilon_{\phi\zeta}^{\zeta\eta\kappa\xi} \epsilon_\phi^*(p_2) p_{2\eta}(k_{1\kappa} + q_\kappa)] \\ & \times [2f_{\mathcal{D} \mathcal{D}^* \phi} \epsilon_{\phi\lambda}^{\lambda\rho\delta\sigma} \epsilon_\phi^*(p_3) p_{3\rho}(q_\delta - k_{2\delta})], \end{aligned} \quad (29)$$

$$\begin{aligned} \mathcal{M}_{(0-3)} = & \int \frac{d^4 q}{(2\pi)^4} \frac{\tilde{g}_\xi^\mu(k_1)}{k_1^2 - m_{D^*}^2} \frac{\tilde{g}_{\mu\sigma}(k_2)}{k_2^2 - m_{D^*}^2} \frac{1}{q^2 - m_D^2} \mathcal{F}^2(q^2) \\ & \times [-g_{\chi_{c0} \mathcal{D}^* \mathcal{D}^*}] [2f_{\mathcal{D} \mathcal{D}^* \phi} \epsilon_{\phi\zeta}^{\zeta\eta\kappa\xi} \epsilon_\phi^*(p_2) p_{2\eta}(k_{1\kappa} + q_\kappa)] \\ & \times [-2f_{\mathcal{D} \mathcal{D}^* \phi} \epsilon_{\phi\lambda}^{\lambda\rho\delta\sigma} \epsilon_\phi^*(p_3) p_{3\rho}(q_\delta - k_{2\delta})], \end{aligned} \quad (30)$$

$$\begin{aligned} \mathcal{M}_{(0-4)} = & \int \frac{d^4 q}{(2\pi)^4} \frac{\tilde{g}^{\mu\nu}(k_1)}{k_1^2 - m_{D^*}^2} \frac{\tilde{g}_\mu^t(k_2)}{k_2^2 - m_{D^*}^2} \frac{\tilde{g}^{\nu\sigma}(q)}{q^2 - m_{D^*}^2} \mathcal{F}^2(q^2) \\ & \times [-g_{\chi_{c0} \mathcal{D}^* \mathcal{D}^*}] [g_{\mathcal{D}^* \mathcal{D}^* \psi} g_{\eta\gamma} g_\psi^\eta (k_{1\zeta} + q_\zeta) \\ & - 4f_{\mathcal{D}^* \mathcal{D}^* \phi} p_2^\eta (g_{\gamma\eta} g_{\psi\zeta} - g_{\gamma\zeta} g_{\psi\eta})] \epsilon_\phi^{\zeta\eta}(p_2) \\ & \times [g_{\mathcal{D}^* \mathcal{D}^* \phi} g_{\rho\lambda} g_\nu^\rho (q_\lambda - k_{2\lambda}) - 4f_{\mathcal{D}^* \mathcal{D}^* \phi} p_3^\rho \\ & \times (g_{\rho\lambda} g_{\nu\lambda} - g_{\lambda\lambda} g_{\nu\rho})] \epsilon_\phi^{\lambda\rho}(p_3), \end{aligned} \quad (31)$$

In the similar way, the amplitudes of $\chi_{c1} \rightarrow \phi\phi$ and $\chi_{c2} \rightarrow \phi\phi$ can be written out, which are collected into Appendix D and Appendix E, respectively.

In the amplitudes of $\chi_{cJ} \rightarrow \phi\phi$ transitions, a dipole form factor $\mathcal{F}(q^2) = (m_E^2 - \Lambda^2)/(q^2 - \Lambda^2)^2$ is introduced to reflect the structure effect of interaction vertices and the off-shell effect of exchanged mesons [7]. In the expression of $\mathcal{F}(q^2)$, m_E is the mass of the exchanged $\mathcal{D}^{(*)}$ and Λ denotes the cutoff, which is usually parameterized as $\Lambda = m_E + \alpha_\Lambda \Lambda_{\text{QCD}}$ with $\Lambda_{\text{QCD}} = 0.22 \text{ GeV}$ [3, 10–20].

With Eqs. (28–31), considering charge conjugation and isospin symmetries, the polarized amplitudes of $\chi_{cJ} \rightarrow \phi\phi$ read as

$$\mathcal{M}_J(i, \lambda_1, \lambda_2) = 4 \sum_j \mathcal{M}_{(J-j)}^q + 2 \sum_j \mathcal{M}_{(J-j)}^s, \quad (32)$$

where i, λ_1 and λ_2 denote the helicities of χ_{cJ} and two ϕ mesons, respectively, $\mathcal{M}_{(J-j)}^q$ and $\mathcal{M}_{(J-j)}^s$ represent that the triangle loops are composed of charmed and charmed-strange mesons, respectively.

Thus, the helicity amplitudes can be calculated by the following expression

$$|F_{\lambda_1, \lambda_2}^{(J)}|^2 = \sum_i \rho_J(i) |\mathcal{M}_J(i, \lambda_1, \lambda_2)|^2, \quad (33)$$

where ρ_J is the SDM given in Sec. II, i.e.,

$$\rho_0 = 1, \quad (34)$$

$$\rho_1 = \frac{1}{4} \text{diag}\{1, 2, 1\}, \quad (35)$$

$$\rho_2 = \frac{3}{20} \text{diag}\{2, 1, \frac{2}{3}, 1, 2\}. \quad (36)$$

Finally, the general expression of the decay widths of $\chi_{cJ} \rightarrow \phi\phi$ processes reads as

$$\Gamma_{\chi_{cJ} \rightarrow \phi\phi} = \frac{1}{1 + \delta} \frac{1}{\sum_i \rho_J(i)} \frac{1}{8\pi m_{\chi_{cJ}}^2} \sum_{i, \lambda_1, \lambda_2} |\mathcal{M}_J(i, \lambda_1, \lambda_2)|^2, \quad (37)$$

where factor δ should be introduced if the final states are identical particles. Thus, for the discussed $\chi_{cJ} \rightarrow \phi\phi$ transitions, we should take $\delta = 1$.

IV. NUMERICAL RESULTS

A. Helicity amplitudes

With the formula given in Sec. III, now we can estimate all the helicity amplitudes $F_{\lambda_1, \lambda_2}^{(J)}$. Besides the masses taken from the Particle Data Group (PDG) [35], other input parameters include the coupling constants, the mixing angle θ between ω^p and ϕ^p , and the parameter α_Λ that appears in the expression of form factor $\mathcal{F}(q^2)$. For the coupling constants relevant to the interactions between χ_{cJ} and $D_{(s)}^{(*)} \bar{D}_{(s)}^{(*)}$, in the heavy quark limit, they are related to one gauge coupling constant g_1 given in Eq. (18), i.e.,

$$g_{\chi_{c0} \mathcal{D} \mathcal{D}} = 2\sqrt{3}g_1 \sqrt{m_{\chi_{c0}} m_{\mathcal{D}}}, \quad g_{\chi_{c0} \mathcal{D}^* \mathcal{D}^*} = \frac{2}{\sqrt{3}}g_1 \sqrt{m_{\chi_{c0}} m_{\mathcal{D}^*}},$$

$$g_{\chi_{c1} \mathcal{D} \mathcal{D}^*} = 2\sqrt{2}g_1 \sqrt{m_{\chi_{c1}} m_{\mathcal{D}} m_{\mathcal{D}^*}}, \quad g_{\chi_{c2} \mathcal{D} \mathcal{D}} = 2g_1 \frac{\sqrt{m_{\chi_{c0}}}}{m_{\mathcal{D}}},$$

$$g_{\chi_{c2} \mathcal{D} \mathcal{D}^*} = g_1 \sqrt{\frac{m_{\chi_{c2}}}{m_{\mathcal{D}}^3 m_{\mathcal{D}}}}, \quad g_{\chi_{c2} \mathcal{D}^* \mathcal{D}^*} = 4g_1 \sqrt{m_{\chi_{c2}} m_{\mathcal{D}^*}},$$

where $g_1 = -\sqrt{\frac{m_{\chi_{c0}}}{3}} \frac{1}{f_{\chi_{c0}}}$ is from Refs. [10, 22] and $f_{\chi_{c0}} = 0.51 \text{ GeV}$ is the decay constant of χ_{c0} [10, 22]. Similarly, the coupling constants of $D_{(s)}^{(*)} \bar{D}_{(s)}^{(*)} \phi$ interactions can be extracted from Eq. (21)

$$g_{D_s D_s \phi} = g_{D_s^* D_s^* \phi} = \frac{\beta g_V}{\sqrt{2}} \sigma,$$

$$f_{D_s D_s^* \phi} = \frac{f_{D_s^* D_s^* \phi}}{m_{D_s^*}} = \frac{\lambda g_V}{\sqrt{2}} \sigma,$$

$$g_{D D \phi} = g_{D^* D^* \phi} = \frac{\beta g_V}{\sqrt{2}} \zeta,$$

$$f_{D D^* \phi} = \frac{f_{D^* D^* \phi}}{m_{D^*}} = \frac{\lambda g_V}{\sqrt{2}} \zeta$$

with $\beta = 0.9$ and $\lambda = 0.56 \text{ GeV}^{-1}$. Additionally, we have $g_V = m_\rho/f_\pi$ associated with the pion decay constant $f_\pi = 132 \text{ MeV}$ [30–33].

For the mixing angle θ between ω^p and ϕ^p , since the experimental measurement of the branching ratio of the double-OZI suppressed process $\chi_{c1} \rightarrow \omega\phi$ is not zero [1, 2], the mixing of ω^p and ϕ^p should not be ideal, i.e., $\theta \neq 0$. Thus, following the results of Refs. [7, 36–38], in this work we also set $\theta = (3.4 \pm 0.2)^\circ$ to calculate the helicity amplitudes $F_{\lambda_1, \lambda_2}^{(J)}$.

Then, by using the experimental data of the branching ratios of $\chi_{cJ} \rightarrow \phi\phi$ processes, the value α_Λ can be determined. During our calculation, we find that to reproduce all the branching ratios $\mathcal{B}(\chi_{cJ} \rightarrow \phi\phi)$ given by PDG [35] simultaneously, α_Λ should be in the interval [1.15, 1.35], which obeys the requirement that the cutoff Λ should not be too far away from the physical mass of the exchanged mesons [20] and is consistent with the value given by [7].

With the above preparations, finally it is very exciting for us to find that the ratios between these helicity amplitudes are quiet stable when changing α_Λ and θ , which are different from the behavior of individual $F_{\lambda_1, \lambda_2}^{(J)}$. When scanning $\alpha_\Lambda \in [1.15, 1.35]$ and $\theta = (3.4 \pm 0.2)^\circ$ ranges, we get

$$\left| \frac{F_{1,1}^{(0)}}{F_{0,0}^{(0)}} \right| = 0.359 \pm 0.019, \quad (38)$$

for the $\chi_{c0} \rightarrow \phi\phi$ decay,

$$\left| \frac{F_{1,0}^{(1)}}{F_{0,1}^{(1)}} \right| = 1, \quad (39)$$

$$\left| \frac{F_{1,1}^{(1)}}{F_{0,1}^{(1)}} \right| = 0, \quad (40)$$

for the $\chi_{c1} \rightarrow \phi\phi$ decay, and

$$\left| \frac{F_{1,0}^{(2)}}{F_{0,0}^{(2)}} \right| = \left| \frac{F_{0,1}^{(2)}}{F_{0,0}^{(2)}} \right| = 1.285 \pm 0.017, \quad (41)$$

$$\left| \frac{F_{1,-1}^{(2)}}{F_{0,0}^{(2)}} \right| = \left| \frac{F_{-1,1}^{(2)}}{F_{0,0}^{(2)}} \right| = 5.110 \pm 0.057, \quad (42)$$

$$\left| \frac{F_{-1,-1}^{(2)}}{F_{0,0}^{(2)}} \right| = \left| \frac{F_{1,1}^{(2)}}{F_{0,0}^{(2)}} \right| = 0.465 \pm 0.002. \quad (43)$$

for the $\chi_{c2} \rightarrow \phi\phi$ case.

Thus, these ratios of helicity amplitude receives the long distance contributions and characterize the loop effects in the $\chi_{cJ} \rightarrow \phi\phi$ decays. We expect that they can be measured in the future, and used for testing the hadron loop mechanism.

B. Polarization observables

Apart from the directly measurements on the ratios given in Sec. IV A, the t_{ij} moments, $\langle t_{ij} \rangle$, can also be selected as the spin observables, since their distributions are directly related to the helicity amplitude $F_{\lambda_1, \lambda_2}^{(J)}$. The t_{ij} observables are constructed only with the Kaon angles in ϕ decays. Thus, the $\langle t_{ij} \rangle$

moments should be independent on any parameter from theoretical investigations. In experiment, the $\langle t_{ij} \rangle$ moments are defined as

$$\langle t_{ij} \rangle = \frac{1}{I_0} \int t_{ij} |\mathcal{M}|^2 d\Omega_2 d\Omega_3, \quad (44)$$

where $|\mathcal{M}|^2$ denotes the joint angular distribution for the $\chi_{cJ} \rightarrow \phi\phi \rightarrow 2(K^+ K^-)$ decay and $d\Omega_i = d\cos\theta_i d\phi_i$ ($i = 2, 3$) is the angles to be integrated out. I_0 is the normalization factor.

One exception is the $\chi_{c0} \rightarrow \phi\phi$ decay, in which the multipole parameters C_{ij} are independent on the angles of θ_1 or ϕ_1 . Thus, the $\langle t_{ij} \rangle$ moments are uniformly distributed, and they can not be used as observable. Instead, we chose an observable $\mu = \sin^2\theta_2 \sin^2\theta_3$ to express two ϕ spin entanglements produced from the χ_{c0} decays. With the joint angular distribution \mathcal{W}_0 , one has

$$\langle \mu \rangle \propto 1 + 16 |F_{1,1}^{(0)} / F_{0,0}^{(0)}|^2 \cos^2(\phi_2 + \phi_3). \quad (45)$$

An ensemble of events is generated by using the χ_{c0} decay amplitude \mathcal{W}_0 . And the ratio of amplitude is fixed to the central value of calculation, namely, $|F_{1,1}^{(0)} / F_{0,0}^{(0)}| = 0.359$. The $\langle \sin^2\theta_2 \sin^2\theta_3 \rangle$ moment of these TOY Monte-Carlo (MC) events is shown in Fig. 5. One can see that the MC distribution is consistent with the expectation of $1 + 2 \cos^2(\phi_2 + \phi_3)$.

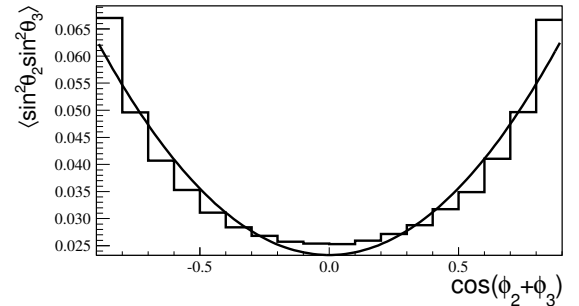


FIG. 5: Distribution of $\langle \sin^2\theta_2 \sin^2\theta_3 \rangle$ moment versus $\cos(\phi_2 + \phi_3)$ for the $\chi_{c0} \rightarrow \phi\phi \rightarrow 2(K^+ K^-)$. Histogram is filled with the MC events, and the curve shows the distribution of $1 + 2 \cos^2(\phi_2 + \phi_3)$.

For the $\chi_{c1} \rightarrow \phi\phi$ decay, it conserves parity and the decay amplitude respects the identical particle symmetry when exchanging two ϕ mesons. Thus, the helicity amplitudes are able to factor out as an overall factor in the angular distribution. The ϕ angular distribution is independent on the amplitudes, and it is reduced to

$$\frac{dN}{d\cos\theta_1} \propto 1 - \frac{1}{3} \cos^2\theta_1, \quad (46)$$

which corresponds to the observation of moment $\langle t_{00} \rangle$ for the $\chi_{c1} \rightarrow \phi\phi$ decay.

We generate an ensemble of MC events for the χ_{c1} decay with the amplitudes constrained by the requirements of parity conservation and the identical particle symmetry, namely,

$F_{1,1}^{(1)} = 0$, $F_{1,0}^{(1)} = -F_{0,1}^{(1)}$. Figure 6 shows the angular distribution for the ϕ meson from the χ_{c1} decays. One can see that the distribution is well consistent with the expected one as given by Eq. (46).

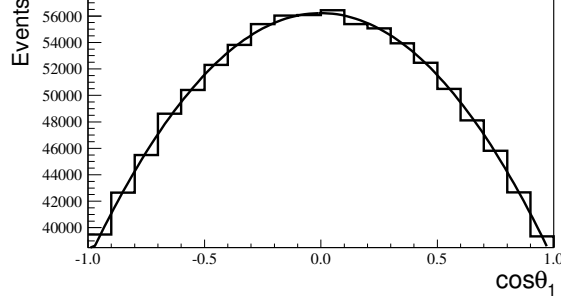


FIG. 6: Angular distribution of ϕ meson in χ_{c1} decays. Histogram is filled with the MC events, and the curve shows the distribution of $1 - \frac{1}{3} \cos^2 \theta_1$.

One significant feature of t_{ij} moments for χ_{c1} decays is that their distributions are well determined only with the fundamental conservation rule and symmetry relations, being independent on the helicity amplitudes $F_{\lambda_1, \lambda_2}^{(1)}$. For example, some $\langle t_{ij} \rangle$ moments are determined to be

$$\langle t_{55} \rangle \propto 1 - \frac{1}{2} \cos^2 \theta_1, \quad (47)$$

$$\langle t_{60} \rangle, \langle t_{06} \rangle, \langle t_{66} \rangle \propto 1 - \frac{1}{3} \cos^2 \theta_1, \quad (48)$$

$$\langle t_{80} \rangle, \langle t_{08} \rangle, \langle t_{68} \rangle, \langle t_{86} \rangle \propto 1 - \cos^2 \theta_1. \quad (49)$$

Figure 7 shows the $\langle t_{55} \rangle$ moment distribution filled with the χ_{c1} MC events. The curve shows the expected distribution, and it is well consistent with the MC events.

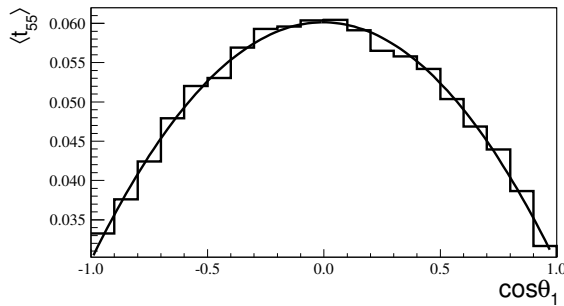


FIG. 7: Moment distribution of $\langle t_{55} \rangle$ for χ_{c1} decays. Histogram is filled with the MC events, and the curve shows the distribution of $1 - \frac{1}{2} \cos^2 \theta_1$.

To show the $\langle t_{ij} \rangle$ moments for the $\chi_{c2} \rightarrow \phi\phi \rightarrow 2(K^+K^-)$ decay, we generated MC events with the central values of predicted amplitude ratios, i.e. $|F_{1,0}^{(2)}|/|F_{0,0}^{(2)}| = |F_{0,1}^{(2)}|/|F_{0,0}^{(2)}| = 1.285$, $|F_{1,-1}^{(2)}|/|F_{0,0}^{(2)}| = |F_{-1,1}^{(2)}|/|F_{0,0}^{(2)}| = 5.11$ and $|F_{1,1}^{(2)}|/|F_{0,0}^{(2)}| =$

0.465. The $\langle t_{00} \rangle$ moments corresponds to the ϕ meson angular distribution. It reads as

$$\frac{dN}{d \cos \theta_1} \propto 1 + \alpha \cos^2 \theta_1 \quad (50)$$

with the angular distribution parameter

$$\alpha = - \frac{3 \left[|F_{0,0}^{(2)}|^2 + 2 \left(-|F_{1,-1}^{(2)}|^2 + |F_{1,0}^{(2)}|^2 + |F_{1,1}^{(2)}|^2 \right) \right]}{5|F_{0,0}^{(2)}|^2 + 6|F_{1,-1}^{(2)}|^2 + 18|F_{1,0}^{(2)}|^2 + 10|F_{1,1}^{(2)}|^2}. \quad (51)$$

Using the amplitude ratios, one has $\alpha = 0.736$. Figure 8 shows the angular distribution (histogram) for the ϕ meson filled with the MC events, and the comparison with the predicted angular distribution (curve).

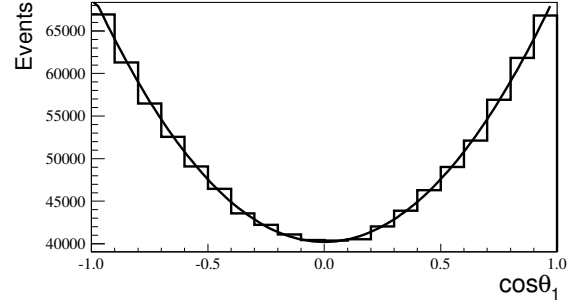


FIG. 8: Angular distribution of the ϕ meson for χ_{c2} decays. Histogram is filled with the MC events, and the curve shows the distribution of $1 + 0.736 \cos^2 \theta_1$.

Another moment, $\langle t_{06} \rangle$ or $\langle t_{60} \rangle$, can also be used to reveal the amplitude ratios. It distributes with the form $\langle t_{06} \rangle \propto 1 + \alpha_1 \cos^2 \theta_1$ with

$$\alpha_1 = - \frac{3 \left(2|F_{0,0}^{(2)}|^2 + 2|F_{1,-1}^{(2)}|^2 + |F_{1,0}^{(2)}|^2 - 2|F_{1,1}^{(2)}|^2 \right)}{10|F_{0,0}^{(2)}|^2 - 6|F_{1,-1}^{(2)}|^2 + 9|F_{1,0}^{(2)}|^2 - 10|F_{1,1}^{(2)}|^2}. \quad (52)$$

Using the predicted amplitude ratios, we get $\alpha_1 = 1.24$. Figure 9 shows the $\langle t_{06} \rangle$ distribution, filled with the MC events, which is comparable with the predicted distribution with $\alpha_1 = 1.24$.

There are some $\langle t_{ij} \rangle$ moments in the χ_{c2} decays, distributing independently on the amplitude ratios. After factoring out the amplitudes, we obtain these moment distributions versus $x = \cos \theta_1$, i.e.,

$$\langle t_{44} \rangle \propto 1 - 6x^2/10, \quad (53)$$

$$\langle t_{76} \rangle, \langle t_{67} \rangle \propto x \sqrt{1 - x^2}, \quad (54)$$

$$\langle t_{80} \rangle, \langle t_{08} \rangle \propto 1 - x^2. \quad (55)$$

Figure 10 shows the $\langle t_{76} \rangle$ distribution, for example, for χ_{c2} decays, and the comparison with the predicted one.

V. SUMMARY

The anomalous decay behaviors of the $\chi_{cJ} \rightarrow VV$ ($VV = \omega\omega, \omega\phi$ and $\phi\phi$) transitions [1, 2] indicate that the non-perturbative effect of strong interaction cannot be ignored.

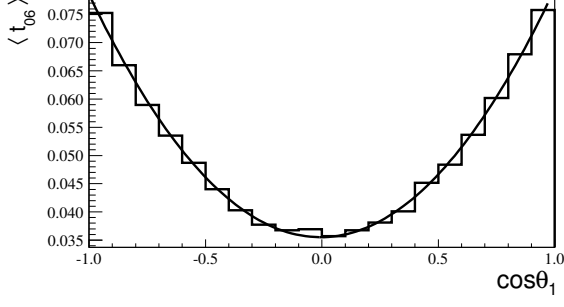


FIG. 9: Angular distribution of the ϕ meson for χ_{c2} decays. Histogram is filled with the MC events, and the curve shows the distribution of $1 + 1.26 \cos^2 \theta_1$.

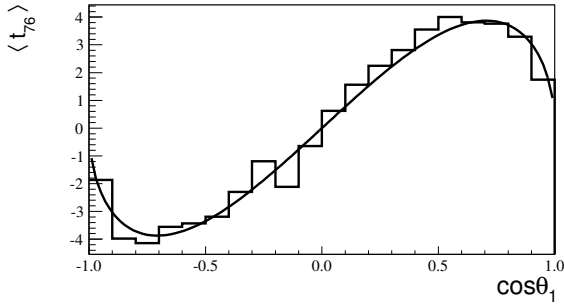


FIG. 10: Distribution of the $\langle t_{76} \rangle$ moment for χ_{c2} decays. Histogram is filled with the MC events, and the curve shows the distribution of $x \sqrt{1 - x^2}$ with $x = \cos \theta_1$.

For reflecting non-perturbative effect of strong interaction, hadronic loop mechanism is adopted to study the branching ratios of $\chi_{cJ} \rightarrow VV$ ($VV = \omega\omega$, $\omega\phi$ and $\phi\phi$) processes [6, 7]. Although the measured branching ratios of the $\chi_{c1} \rightarrow \omega\omega$ and $\chi_{c1} \rightarrow \phi\phi$ processes can be reproduced well, it is not the end of whole story. In fact, we still want to find more crucial information to reflect the evidence of the hadronic loop mechanism existing in the $\chi_{cJ} \rightarrow \omega\phi$ processes [1, 2].

Inspired by Refs. [7, 39, 40], we propose that the polarization information of the $\chi_{cJ} \rightarrow VV$ decay can be applied to probe the hadronic loop mechanism, which becomes main task of this work. The advantage to choose the $\chi_{cJ} \rightarrow \phi\phi$ decay is due to the factor that two ϕ decays provide a rich spin observables. Another advantage is that these decays are accessible in experiment with high detection efficiency and two ϕ mesons are cleanly reconstructed with low level backgrounds. A high statistics allow one to perform the angular distribution analyses and get the information on the ϕ polarization, which can shed light on the underlying decay mechanism for the $\chi_{cJ} \rightarrow VV$ decays.

Under the framework of hadronic loop mechanism, we find that the ratios of the helicity amplitudes of the $\chi_{cJ} \rightarrow \phi\phi$ processes are quiet stable, where we scan the ranges of θ and α_Λ , which are the mixing angle between ω^P and ϕ^P and the free parameter of the form factor, respectively. Thus, we suggest that

these ratios can be as important observable quantities, which can be accessible at future experimental measurement as crucial test to hadronic loop mechanism.

In addition, by using the predicted amplitude ratios, we show that the observation of moments $\langle t_{ij} \rangle$ can be used to manifest the nontrivial polarization behavior. For the χ_{c0} decays, the choice of the spin observable is quite limited due to the fact that the total spin of the $\phi\phi$ system is constrained to be zero in the spin triplet. Thus, the spins of two ϕ mesons are antiparallel for the χ_{c0} decays. For the $\chi_{c1} \rightarrow \phi\phi$ decays, the helicity amplitudes can be well determined by considering parity conservation and by applying the symmetry relationship to take the $\phi\phi$ as identical particle system. For the $\chi_{c2} \rightarrow \phi\phi$ decays, the abundant information of the $\phi\phi$ spin configurations allows us to directly detect the helicity amplitudes from the observation of different $\langle t_{ij} \rangle$ moments. The patterns of these moments are presented based on the predicted amplitude ratios, which can be tested by experiment in the near future.

In 2019, BESIII released white paper on its future physics program [41]. With the accumulation of charmonium data, we suggest that BESIII should pay more attentions to the study of polarization of the corresponding decays, which may provide extra information to reveal underlying mechanism. Obviously, the present work provides a typical example and a new task for experiment.

Acknowledgments

This work is supported by the China National Funds for Distinguished Young Scientists under Grant No. 11825503, National Key Research and Development Program of China under Contract No. 2020YFA0406400, the 111 Project under Grant No. B20063, and the National Natural Science Foundation of China under Grant No. 12047501, 11875262 and 11835012.

Appendix A SPIN OBSERVABLE t_{ij} .

The obtained spin observables t_{ij} are

$$\begin{aligned}
t_{00} &= \frac{1}{9}, \\
t_{40} &= -\frac{\sin^2(\theta_2) \sin(2\phi_2)}{3\sqrt{3}}, \\
t_{04} &= -\frac{\sin^2(\theta_3) \sin(2\phi_3)}{3\sqrt{3}}, \\
t_{44} &= \frac{1}{3} \sin^2(\theta_2) \sin^2(\theta_3) \sin(2\phi_2) \sin(2\phi_3), \\
t_{45} &= \frac{1}{3} \sin^2(\theta_2) \sin(2\theta_3) \sin(2\phi_2) \sin(\phi_3), \\
t_{46} &= \frac{\sin^2(\theta_2) (3 \cos(2\theta_3) + 1) \sin(2\phi_2)}{6\sqrt{3}}, \\
t_{47} &= \frac{1}{3} \sin^2(\theta_2) \sin(2\theta_3) \sin(2\phi_2) \cos(\phi_3), \\
t_{48} &= \frac{1}{3} \sin^2(\theta_2) \sin^2(\theta_3) \sin(2\phi_2) \cos(2\phi_3), \\
t_{50} &= -\frac{\sin(2\theta_2) \sin(\phi_2)}{3\sqrt{3}}, \\
t_{05} &= -\frac{\sin(2\theta_3) \sin(\phi_3)}{3\sqrt{3}}, \\
t_{54} &= \frac{1}{3} \sin(2\theta_2) \sin^2(\theta_3) \sin(\phi_2) \sin(2\phi_3), \\
t_{55} &= \frac{1}{3} \sin(2\theta_2) \sin(2\theta_3) \sin(\phi_2) \sin(\phi_3), \\
t_{56} &= \frac{\sin(2\theta_2) (3 \cos(2\theta_3) + 1) \sin(\phi_2)}{6\sqrt{3}}, \\
t_{57} &= \frac{1}{3} \sin(2\theta_2) \sin(2\theta_3) \sin(\phi_2) \cos(\phi_3), \\
t_{58} &= \frac{1}{3} \sin(2\theta_2) \sin^2(\theta_3) \sin(\phi_2) \cos(2\phi_3), \\
t_{60} &= \frac{1}{18} (-3 \cos(2\theta_2) - 1), \\
t_{06} &= \frac{1}{18} (-3 \cos(2\theta_3) - 1), \\
t_{64} &= \frac{\sin^2(\theta_3) (3 \cos(2\theta_2) + 1) \sin(2\phi_3)}{6\sqrt{3}}, \\
t_{65} &= \frac{\sin(2\theta_3) (3 \cos(2\theta_2) + 1) \sin(\phi_3)}{6\sqrt{3}}, \\
t_{66} &= \frac{1}{36} (3 \cos(2\theta_2) + 1) (3 \cos(2\theta_3) + 1), \\
t_{67} &= \frac{\sin(2\theta_3) (3 \cos(2\theta_2) + 1) \cos(\phi_3)}{6\sqrt{3}}, \\
t_{68} &= \frac{\sin^2(\theta_3) (3 \cos(2\theta_2) + 1) \cos(2\phi_3)}{6\sqrt{3}}, \\
t_{70} &= -\frac{\sin(2\theta_2) \cos(\phi_2)}{3\sqrt{3}}, \\
t_{07} &= -\frac{\sin(2\theta_3) \cos(\phi_3)}{3\sqrt{3}}, \\
t_{74} &= \frac{1}{3} \sin(2\theta_2) \sin^2(\theta_3) \sin(2\phi_3) \cos(\phi_2),
\end{aligned}$$

$$\begin{aligned}
t_{75} &= \frac{1}{3} \sin(2\theta_2) \sin(2\theta_3) \sin(\phi_3) \cos(\phi_2), \\
t_{76} &= \frac{\sin(2\theta_2) (3 \cos(2\theta_3) + 1) \cos(\phi_2)}{6\sqrt{3}}, \\
t_{77} &= \frac{1}{3} \sin(2\theta_2) \sin(2\theta_3) \cos(\phi_2) \cos(\phi_3), \\
t_{78} &= \frac{1}{3} \sin(2\theta_2) \sin^2(\theta_3) \cos(\phi_2) \cos(2\phi_3), \\
t_{80} &= -\frac{\sin^2(\theta_2) \cos(2\phi_2)}{3\sqrt{3}}, \\
t_{08} &= -\frac{\sin^2(\theta_3) \cos(2\phi_3)}{3\sqrt{3}}, \\
t_{84} &= \frac{1}{3} \sin^2(\theta_2) \sin^2(\theta_3) \sin(2\phi_3) \cos(2\phi_2), \\
t_{85} &= \frac{1}{3} \sin^2(\theta_2) \sin(2\theta_3) \sin(\phi_3) \cos(2\phi_2), \\
t_{86} &= \frac{\sin^2(\theta_2) (3 \cos(2\theta_3) + 1) \cos(2\phi_2)}{6\sqrt{3}}, \\
t_{87} &= \frac{1}{3} \sin^2(\theta_2) \sin(2\theta_3) \cos(2\phi_2) \cos(\phi_3), \\
t_{88} &= \frac{1}{3} \sin^2(\theta_2) \sin^2(\theta_3) \cos(2\phi_2) \cos(2\phi_3).
\end{aligned}$$

Appendix B MULTIPOLE PARAMETERS FOR $\chi_{c1} \rightarrow \phi\phi$

We collected the multipole parameters for $\chi_{c1} \rightarrow \phi\phi$, i.e.,

$$\begin{aligned}
C_{00} &= \frac{9}{8} \left(-(\cos(2\theta_1) - 5) |F_{0,1}^{(1)}|^2 \right. \\
&\quad \left. - (\cos(2\theta_1) - 5) |F_{1,0}^{(1)}|^2 + 2(\cos(2\theta_1) + 3) |F_{1,1}^{(1)}|^2 \right), \\
C_{54} &= \frac{3}{32} \sin(2\theta_1) (F_{1,1}^{(1)*} F_{0,1}^{(1)} + F_{0,1}^{(1)*} F_{1,1}^{(1)}), \\
C_{55} &= \frac{3}{32} (\cos(2\theta_1) - 3) (F_{1,0}^{(1)*} F_{0,1}^{(1)} + F_{0,1}^{(1)*} F_{1,0}^{(1)}), \\
C_{60} &= \frac{1}{16} \left(2(\cos(2\theta_1) - 5) |F_{0,1}^{(1)}|^2 - (\cos(2\theta_1) - 5) |F_{1,0}^{(1)}|^2 \right. \\
&\quad \left. + 2(\cos(2\theta_1) + 3) |F_{1,1}^{(1)}|^2 \right), \\
C_{06} &= \frac{1}{16} \left(2((\cos(2\theta_1) - 5) |F_{1,0}^{(1)}|^2 + (\cos(2\theta_1) + 3) |F_{1,1}^{(1)}|^2) \right. \\
&\quad \left. - (\cos(2\theta_1) - 5) |F_{0,1}^{(1)}|^2 \right), \\
C_{66} &= \frac{1}{16} \left((\cos(2\theta_1) - 5) |F_{0,1}^{(1)}|^2 + (\cos(2\theta_1) - 5) |F_{1,0}^{(1)}|^2 \right. \\
&\quad \left. + (\cos(2\theta_1) + 3) |F_{1,1}^{(1)}|^2 \right),
\end{aligned}$$

$$\begin{aligned}
C_{67} &= \frac{1}{32} \sqrt{3} \sin(2\theta_1) (F_{1,1}^{(1)*} F_{1,0}^{(1)} + F_{1,0}^{(1)*} F_{1,1}^{(1)}), \\
C_{68} &= -\frac{1}{8} \sqrt{3} \sin^2(\theta_1) |F_{0,1}^{(1)}|^2, \\
C_{70} &= -\frac{1}{16} \sqrt{3} \sin(2\theta_1) (F_{1,1}^{(1)*} F_{0,1}^{(1)} + F_{0,1}^{(1)*} F_{1,1}^{(1)}), \\
C_{07} &= \frac{1}{16} \sqrt{3} \sin(2\theta_1) (F_{1,1}^{(1)*} F_{1,0}^{(1)} + F_{1,0}^{(1)*} F_{1,1}^{(1)}), \\
C_{76} &= -\frac{1}{32} \sqrt{3} \sin(2\theta_1) (F_{1,1}^{(1)*} F_{0,1}^{(1)} + F_{0,1}^{(1)*} F_{1,1}^{(1)}), \\
C_{77} &= \frac{3}{16} (F_{1,0}^{(1)*} F_{0,1}^{(1)} + F_{0,1}^{(1)*} F_{1,0}^{(1)}), \\
C_{78} &= -\frac{3}{32} \sin(2\theta_1) (F_{1,1}^{(1)*} F_{0,1}^{(1)} + F_{0,1}^{(1)*} F_{1,1}^{(1)}), \\
C_{80} &= \frac{1}{8} \sqrt{3} \sin^2(\theta_1) |F_{1,0}^{(1)}|^2, \\
C_{08} &= \frac{1}{8} \sqrt{3} \sin^2(\theta_1) |F_{0,1}^{(1)}|^2, \\
C_{86} &= -\frac{1}{8} \sqrt{3} \sin^2(\theta_1) |F_{1,0}^{(1)}|^2, \\
C_{87} &= \frac{3}{32} \sin(2\theta_1) (F_{1,1}^{(1)*} F_{1,0}^{(1)} + F_{1,0}^{(1)*} F_{1,1}^{(1)}), \\
C_{88} &= -\frac{3}{16} (\cos(2\theta_1) + 3) |F_{1,1}^{(1)}|^2.
\end{aligned}$$

Appendix C MULTIPOLE PARAMETERS FOR $\chi_{c2} \rightarrow \phi\phi$

The multipole parameters for $\chi_{c2} \rightarrow \phi\phi$ are

$$\begin{aligned}
C_{00} &= \frac{9}{40} [-3 \cos(2\theta_1) \\
&\times (|F_{1,0}^{(2)}|^2 + 2 |F_{1,1}^{(2)}|^2 + F_{1,0}^{(2)*} F_{0,1}^{(2)} - F_{-1,1}^{(2)*} F_{1,-1}^{(2)}) \\
&+ (7 - 3 \cos(2\theta_1)) |F_{0,0}^{(2)}|^2 + 3 (\cos(2\theta_1) + 3) |F_{1,-1}^{(2)}|^2 \\
&+ 15 |F_{1,0}^{(2)}|^2 + 14 |F_{1,1}^{(2)}|^2 + 15 F_{1,0}^{(2)*} F_{0,1}^{(2)} + 9 F_{-1,1}^{(2)*} F_{1,-1}^{(2)}], \\
C_{44} &= \frac{3}{80} (3 \cos(2\theta_1) - 7) |F_{1,1}^{(2)}|^2, \\
C_{45} &= -\frac{3}{160} \sqrt{3} \sin(2\theta_1) (F_{1,1}^{(2)*} F_{1,0}^{(2)} + F_{1,0}^{(2)*} F_{1,1}^{(2)}), \\
C_{54} &= \frac{3}{160} \sqrt{3} \sin(2\theta_1) (F_{1,1}^{(2)*} F_{1,0}^{(2)} + F_{1,0}^{(2)*} F_{1,1}^{(2)}), \\
C_{55} &= -\frac{3}{160} (6 (\cos(2\theta_1) - 3) |F_{1,0}^{(2)}|^2 \\
&+ \sqrt{6} \sin^2(\theta_1) (F_{1,-1}^{(2)*} F_{0,0}^{(2)} + F_{0,0}^{(2)*} F_{1,-1}^{(2)}) \\
&- (3 \cos(2\theta_1) - 7) (F_{1,1}^{(2)*} F_{0,0}^{(2)} + F_{0,0}^{(2)*} F_{1,1}^{(2)})),
\end{aligned} \tag{56}$$

$$\begin{aligned}
C_{60} &= \frac{1}{40} ((3 \cos(2\theta_1) - 7) |F_{0,0}^{(2)}|^2 + (7 - 3 \cos(2\theta_1)) |F_{1,1}^{(2)}|^2 \\
&+ 3 (\cos(2\theta_1) + 3) |F_{1,-1}^{(2)}|^2), \\
C_{06} &= \frac{1}{40} ((3 \cos(2\theta_1) - 7) |F_{0,0}^{(2)}|^2 + (7 - 3 \cos(2\theta_1)) |F_{1,1}^{(2)}|^2 \\
&+ 3 (\cos(2\theta_1) + 3) |F_{1,-1}^{(2)}|^2), \\
C_{66} &= \frac{1}{80} (2 (7 - 3 \cos(2\theta_1)) |F_{0,0}^{(2)}|^2 + (7 - 3 \cos(2\theta_1)) |F_{1,1}^{(2)}|^2 \\
&+ 6 (\cos(2\theta_1) - 5) |F_{1,0}^{(2)}|^2 + 3 (\cos(2\theta_1) + 3) |F_{1,-1}^{(2)}|^2), \\
C_{67} &= -\frac{3}{160} \sin(2\theta_1) ((2 F_{0,0}^{(2)*} - \sqrt{6} F_{1,-1}^{(2)*} + F_{1,1}^{(2)*}) F_{1,0}^{(2)} \\
&+ F_{1,0}^{(2)*} (2 F_{0,0}^{(2)} - \sqrt{6} F_{1,-1}^{(2)} + F_{1,1}^{(2)})), \\
C_{68} &= \frac{3}{80} \sin^2(\theta_1) (\sqrt{2} (F_{1,1}^{(2)*} F_{1,-1}^{(2)} + F_{1,-1}^{(2)*} F_{1,1}^{(2)}) - 2 \sqrt{3} |F_{1,0}^{(2)}|^2), \\
C_{76} &= \frac{3}{160} \sin(2\theta_1) ((2 F_{0,0}^{(2)*} - \sqrt{6} F_{1,-1}^{(2)*} + F_{1,1}^{(2)*}) F_{1,0}^{(2)} \\
&+ F_{1,0}^{(2)*} (2 F_{0,0}^{(2)} - \sqrt{6} F_{1,-1}^{(2)} + F_{1,1}^{(2)})), \\
C_{77} &= -\frac{3}{160} (12 |F_{1,0}^{(2)}|^2 + \sqrt{6} \sin^2(\theta_1) (F_{1,-1}^{(2)*} F_{0,0}^{(2)} + F_{0,0}^{(2)*} F_{1,-1}^{(2)}) \\
&+ (3 \cos(2\theta_1) - 7) (F_{1,1}^{(2)*} F_{0,0}^{(2)} + F_{0,0}^{(2)*} F_{1,1}^{(2)})), \\
C_{78} &= -\frac{3}{160} \sqrt{3} \sin(2\theta_1) (F_{1,1}^{(2)*} F_{1,0}^{(2)} + F_{1,0}^{(2)*} F_{1,1}^{(2)}), \\
C_{80} &= \frac{3 \sin^2(\theta_1) (F_{1,1}^{(2)*} F_{1,-1}^{(2)} + F_{1,-1}^{(2)*} F_{1,1}^{(2)})}{20 \sqrt{2}}, \\
C_{08} &= \frac{3 \sin^2(\theta_1) (F_{1,1}^{(2)*} F_{1,-1}^{(2)} + F_{1,-1}^{(2)*} F_{1,1}^{(2)})}{20 \sqrt{2}}, \\
C_{86} &= \frac{3}{80} \sin^2(\theta_1) (\sqrt{2} (F_{1,1}^{(2)*} F_{1,-1}^{(2)} + F_{1,-1}^{(2)*} F_{1,1}^{(2)}) - 2 \sqrt{3} |F_{1,0}^{(2)}|^2), \\
C_{87} &= \frac{3}{160} \sqrt{3} \sin(2\theta_1) (F_{1,1}^{(2)*} F_{1,0}^{(2)} + F_{1,0}^{(2)*} F_{1,1}^{(2)}), \\
C_{88} &= -\frac{3}{80} (3 \cos(2\theta_1) - 7) |F_{1,1}^{(2)}|^2.
\end{aligned}$$

Appendix D AMPLITUDES OF $\chi_{c1} \rightarrow \phi\phi$ TRANSITION

For $\chi_{c1} \rightarrow \phi\phi$ transition, the amplitudes corresponding to Fig. (3) are

$$\begin{aligned}
\mathcal{M}_{(1-1)} &= \int \frac{d^4 q}{(2\pi)^4} \frac{\tilde{g}_\xi^\mu(k_1)}{k_1^2 - m_{\mathcal{D}^*}^2} \frac{1}{k_2^2 - m_{\mathcal{D}}^2} \frac{1}{q^2 - m_{\mathcal{D}}^2} \mathcal{F}^2(q^2) \\
&\times [-ig_{\chi_{c1} \mathcal{D} \mathcal{D}^*} \epsilon_{\chi_{c1}}^\mu(p_1)] [-g_{\mathcal{D} \mathcal{D} \phi} \epsilon_{\phi}^{*\lambda}(p_3) (q_\lambda - k_{2\lambda})] \\
&\times [2f_{\mathcal{D} \mathcal{D}^* \phi} \epsilon_{\phi}^{\zeta \eta \kappa \xi} \epsilon_{\phi \zeta}^*(p_2) p_{2\eta} (k_{1\kappa} + q_\kappa)], \tag{58}
\end{aligned}$$

$$\begin{aligned}
\mathcal{M}_{(1-2)} &= \int \frac{d^4 q}{(2\pi)^4} \frac{1}{k_1^2 - m_{\mathcal{D}}^2} \frac{\tilde{g}_{\sigma\mu}(k_2)}{k_2^2 - m_{\mathcal{D}^*}^2} \frac{1}{q^2 - m_{\mathcal{D}}^2} \mathcal{F}^2(q^2) \\
&\times [ig_{\chi_{c1} \mathcal{D} \mathcal{D}^*} \epsilon_{\chi_{c1}}^\mu(p_1)] [-g_{\mathcal{D} \mathcal{D} \phi} \epsilon_{\phi}^{*\zeta}(p_2) (k_{1\zeta} + q_\zeta)] \\
&\times [-2f_{\mathcal{D} \mathcal{D}^* \phi} \epsilon^{\lambda \rho \delta \sigma} \epsilon_{\phi \lambda}^*(p_3) p_{3\rho} (q_\delta - k_{2\delta})], \tag{59}
\end{aligned}$$

$$\begin{aligned}
\mathcal{M}_{(1-3)} = & \int \frac{d^4 q}{(2\pi)^4} \frac{\tilde{g}^{\mu\psi}(k_1)}{k_1^2 - m_{\mathcal{D}}^2} \frac{1}{k_2^2 - m_{\mathcal{D}}^2} \frac{\tilde{g}_\sigma^\gamma(q)}{q^2 - m_{\mathcal{D}^*}^2} \mathcal{F}^2(q^2) \\
& \times [-ig_{\chi_{c1}\mathcal{D}\mathcal{D}^*} \epsilon_{\chi_{c1}}^\mu(p_1)] [g_{\mathcal{D}^*\mathcal{D}^*} \psi g_{\eta\gamma} g_\psi^\eta(k_{1\zeta} + q_\zeta) \\
& - 4f_{\mathcal{D}^*\mathcal{D}^*} p_2^\eta (g_{\gamma\eta} g_{\psi\zeta} - g_{\gamma\zeta} g_{\psi\eta})] \epsilon_\phi^{*\zeta}(p_2) \\
& \times [2f_{\mathcal{D}\mathcal{D}^*} \phi \epsilon^{\lambda\rho\delta\sigma} \epsilon_{\phi\lambda}^*(p_3) p_{3\rho} (q_\delta - k_{2\delta})], \quad (60)
\end{aligned}$$

$$\begin{aligned}
\mathcal{M}_{(1-4)} = & \int \frac{d^4 q}{(2\pi)^4} \frac{1}{k_1^2 - m_{\mathcal{D}}^2} \frac{\tilde{g}^{\mu\mu}(k_2)}{k_2^2 - m_{\mathcal{D}^*}^2} \frac{\tilde{g}_\xi^\nu(q)}{q^2 - m_{\mathcal{D}^*}^2} \mathcal{F}^2(q^2) \\
& \times [-2f_{\mathcal{D}\mathcal{D}^*} \phi \epsilon^{\zeta\eta\kappa\xi} \epsilon_{\phi\zeta}^*(p_2) p_{2\eta} (k_{1\kappa} + q_\kappa)] \\
& \times \epsilon_\phi^{*\lambda}(p_3) [g_{\mathcal{D}^*\mathcal{D}^*} \phi g_{\rho\lambda} g_v^\rho (q_\lambda - k_{2\lambda}) \\
& - 4f_{\mathcal{D}^*\mathcal{D}^*} p_3^\rho (g_{\rho\lambda} g_{v\lambda} - g_{\lambda\lambda} g_{v\rho})] \\
& \times [ig_{\chi_{c1}\mathcal{D}\mathcal{D}^*} \epsilon_{\chi_{c1}}^\mu(p_1)], \quad (61)
\end{aligned}$$

Appendix E AMPLITUDES OF $\chi_{c2} \rightarrow \phi\phi$ TRANSITION

The obtained amplitudes of the $\chi_{c2} \rightarrow \phi\phi$ transition for Fig. (4) are

$$\begin{aligned}
\mathcal{M}_{(2-1)} = & \int \frac{d^4 q}{(2\pi)^4} \frac{1}{k_1^2 - m_{\mathcal{D}}^2} \frac{1}{k_2^2 - m_{\mathcal{D}}^2} \frac{1}{q^2 - m_{\mathcal{D}}^2} \mathcal{F}^2(q^2) \\
& \times [g_{\chi_{c2}\mathcal{D}\mathcal{D}} \epsilon_{\chi_{c2}}^{\mu\nu}(p_1) k_{2\mu} k_{1\nu}] \\
& \times [g_{\mathcal{D}\mathcal{D}\phi} \epsilon_\phi^{*\zeta}(p_2) (k_{1\zeta} + q_\zeta)] \\
& \times [g_{\mathcal{D}\mathcal{D}\phi} \epsilon_\phi^{*\lambda}(p_3) (q_\lambda - k_{2\lambda})], \quad (62)
\end{aligned}$$

$$\begin{aligned}
\mathcal{M}_{(2-2)} = & \int \frac{d^4 q}{(2\pi)^4} \frac{\tilde{g}_\xi^\tau(k_1)}{k_1^2 - m_{\mathcal{D}}^2} \frac{1}{k_2^2 - m_{\mathcal{D}}^2} \frac{1}{q^2 - m_{\mathcal{D}}^2} \mathcal{F}^2(q^2) \\
& \times [-g_{\chi_{c2}\mathcal{D}\mathcal{D}^*} \epsilon_{\mu\tau\alpha\beta} p_1^\alpha \epsilon_{\chi_{c2}}^{\mu\nu}(p_1) k_2^\beta k_{1\nu}] \\
& \times [2f_{\mathcal{D}\mathcal{D}^*} \phi \epsilon^{\zeta\eta\kappa\xi} \epsilon_{\phi\zeta}^*(p_2) p_{2\eta} (k_{1\kappa} + q_\kappa)] \\
& \times [-g_{\mathcal{D}\mathcal{D}\phi} \epsilon_\phi^{*\lambda}(p_3) (q_\lambda - k_{2\lambda})], \quad (63)
\end{aligned}$$

$$\begin{aligned}
\mathcal{M}_{(2-3)} = & \int \frac{d^4 q}{(2\pi)^4} \frac{1}{k_1^2 - m_{\mathcal{D}}^2} \frac{\tilde{g}_\sigma^\tau(k_2)}{k_2^2 - m_{\mathcal{D}^*}^2} \frac{1}{q^2 - m_{\mathcal{D}^*}^2} \mathcal{F}^2(q^2) \\
& \times [-g_{\chi_{c2}\mathcal{D}\mathcal{D}^*} \epsilon_{\mu\tau\alpha\beta} p_1^\alpha \epsilon_{\chi_{c2}}^{\mu\nu}(p_1) k_{2\nu} k_1^\beta] \\
& \times [-g_{\mathcal{D}\mathcal{D}\phi} \epsilon_\phi^{*\zeta}(p_2) (k_{1\zeta} + q_\zeta)] \\
& \times [-2f_{\mathcal{D}\mathcal{D}^*} \phi \epsilon^{\lambda\rho\delta\sigma} \epsilon_{\phi\lambda}^*(p_3) p_{3\rho} (q_\delta - k_{2\delta})], \quad (64)
\end{aligned}$$

$$\begin{aligned}
\mathcal{M}_{(2-4)} = & \int \frac{d^4 q}{(2\pi)^4} \frac{1}{k_1^2 - m_{\mathcal{D}}^2} \frac{1}{k_2^2 - m_{\mathcal{D}}^2} \frac{\tilde{g}_{\xi\sigma}^\gamma(q)}{q^2 - m_{\mathcal{D}^*}^2} \mathcal{F}^2(q^2) \\
& \times [g_{\chi_{c2}\mathcal{D}\mathcal{D}} \epsilon_{\chi_{c2}}^{\mu\nu}(p_1) k_{2\mu} k_{1\nu}] \\
& \times [-2f_{\mathcal{D}\mathcal{D}^*} \phi \epsilon^{\zeta\eta\kappa\xi} \epsilon_{\phi\zeta}^*(p_2) p_{2\eta} (k_{1\kappa} + q_\kappa)] \\
& \times [2f_{\mathcal{D}\mathcal{D}^*} \phi \epsilon^{\lambda\rho\delta\sigma} \epsilon_{\phi\lambda}^*(p_3) p_{3\rho} (q_\delta - k_{2\delta})], \quad (65)
\end{aligned}$$

$$\begin{aligned}
\mathcal{M}_{(2-5)} = & \int \frac{d^4 q}{(2\pi)^4} \frac{\tilde{g}_{\omega\xi}^\gamma(k_1)}{k_1^2 - m_{\mathcal{D}}^2} \frac{\tilde{g}_{\chi\sigma}^\gamma(k_2)}{k_2^2 - m_{\mathcal{D}^*}^2} \frac{1}{q^2 - m_{\mathcal{D}}^2} \mathcal{F}^2(q^2) \\
& \times [g_{\chi_{c2}\mathcal{D}^*\mathcal{D}^*} \epsilon_{\chi_{c2}}^{\mu\nu}(p_1) (g_{\nu\omega} g_{\mu\chi} + g_{\mu\omega} g_{\nu\chi})] \\
& \times [2f_{\mathcal{D}\mathcal{D}^*} \phi \epsilon^{\zeta\eta\kappa\xi} \epsilon_{\phi\zeta}^*(p_2) p_{2\eta} (k_{1\kappa} + q_\kappa)] \\
& \times [-2f_{\mathcal{D}\mathcal{D}^*} \phi \epsilon^{\lambda\rho\delta\sigma} \epsilon_{\phi\lambda}^*(p_3) p_{3\rho} (q_\delta - k_{2\delta})], \quad (66)
\end{aligned}$$

$$\begin{aligned}
\mathcal{M}_{(2-6)} = & \int \frac{d^4 q}{(2\pi)^4} \frac{\tilde{g}^{\tau\psi}(k_1)}{k_1^2 - m_{\mathcal{D}}^2} \frac{1}{k_2^2 - m_{\mathcal{D}}^2} \frac{\tilde{g}_\sigma^\gamma(q)}{q^2 - m_{\mathcal{D}^*}^2} \mathcal{F}^2(q^2) \\
& \times [-g_{\chi_{c2}\mathcal{D}\mathcal{D}^*} \epsilon_{\mu\tau\alpha\beta} p_1^\alpha \epsilon_{\chi_{c2}}^{\mu\nu}(p_1) k_2^\beta k_{1\nu}] \\
& \times \epsilon_\phi^{*\zeta}(p_2) [g_{\mathcal{D}^*\mathcal{D}^*} \psi g_{\eta\gamma} g_\psi^\eta(k_{1\zeta} + q_\zeta) \\
& - 4f_{\mathcal{D}^*\mathcal{D}^*} p_2^\eta (g_{\gamma\eta} g_{\psi\zeta} - g_{\gamma\zeta} g_{\psi\eta})] \\
& \times [2f_{\mathcal{D}\mathcal{D}^*} \phi \epsilon^{\lambda\rho\delta\sigma} \epsilon_{\phi\lambda}^*(p_3) p_{3\rho} (q_\delta - k_{2\delta})], \quad (67)
\end{aligned}$$

$$\begin{aligned}
\mathcal{M}_{(2-7)} = & \int \frac{d^4 q}{(2\pi)^4} \frac{1}{k_1^2 - m_{\mathcal{D}}^2} \frac{\tilde{g}^{\tau\tau}(k_2)}{k_2^2 - m_{\mathcal{D}^*}^2} \frac{\tilde{g}_\xi^\nu(q)}{q^2 - m_{\mathcal{D}^*}^2} \mathcal{F}^2(q^2) \\
& \times [-g_{\chi_{c2}\mathcal{D}\mathcal{D}^*} \epsilon_{\mu\tau\alpha\beta} p_1^\alpha \epsilon_{\chi_{c2}}^{\mu\nu}(p_1) k_{2\nu} k_1^\beta] \\
& \times [-2f_{\mathcal{D}\mathcal{D}^*} \phi \epsilon^{\zeta\eta\kappa\xi} \epsilon_{\phi\zeta}^*(p_2) p_{2\eta} (k_{1\kappa} + q_\kappa)] \\
& \times \epsilon_\phi^{*\lambda}(p_3) [g_{\mathcal{D}^*\mathcal{D}^*} \phi g_{\rho\lambda} g_v^\rho (q_\lambda - k_{2\lambda}) \\
& - 4f_{\mathcal{D}^*\mathcal{D}^*} p_3^\rho (g_{\rho\lambda} g_{v\lambda} - g_{\lambda\lambda} g_{v\rho})], \quad (68)
\end{aligned}$$

$$\begin{aligned}
\mathcal{M}_{(2-8)} = & \int \frac{d^4 q}{(2\pi)^4} \frac{\tilde{g}_\omega^\psi(k_1)}{k_1^2 - m_{\mathcal{D}}^2} \frac{\tilde{g}_\chi^\tau(k_2)}{k_2^2 - m_{\mathcal{D}^*}^2} \frac{\tilde{g}^{\gamma\nu}(q)}{q^2 - m_{\mathcal{D}^*}^2} \mathcal{F}^2(q^2) \\
& \times [g_{\chi_{c2}\mathcal{D}^*\mathcal{D}^*} \epsilon_{\chi_{c2}}^{\mu\nu}(p_1) (g_{\nu\omega} g_{\mu\chi} + g_{\mu\omega} g_{\nu\chi})] \\
& \times \epsilon_\phi^{*\zeta}(p_2) [g_{\mathcal{D}^*\mathcal{D}^*} \psi g_{\eta\gamma} g_\psi^\eta(k_{1\zeta} + q_\zeta) \\
& - 4f_{\mathcal{D}^*\mathcal{D}^*} p_2^\eta (g_{\gamma\eta} g_{\psi\zeta} - g_{\gamma\zeta} g_{\psi\eta})] \\
& \times \epsilon_\phi^{*\lambda}(p_3) [g_{\mathcal{D}^*\mathcal{D}^*} \phi g_{\rho\lambda} g_v^\rho (q_\lambda - k_{2\lambda}) \\
& - 4f_{\mathcal{D}^*\mathcal{D}^*} p_3^\rho (g_{\rho\lambda} g_{v\lambda} - g_{\lambda\lambda} g_{v\rho})]. \quad (69)
\end{aligned}$$

-
- [1] M. Ablikim *et al.* [BESII], Observation of χ_{c1} decays into vector meson pairs $\phi\phi$, $\omega\omega$, and $\omega\phi$, Phys. Rev. Lett. **107**, 092001 (2011).
[2] M. Ablikim *et al.* [BESIII], Observation of OZI-suppressed decays $\chi_{cJ} \rightarrow \omega\phi$, Phys. Rev. D **99**, no.1, 012015 (2019).
[3] X. Liu, X. Q. Zeng and X. Q. Li, Study on contributions of hadronic loops to decays of J/ψ to vector + pseudoscalar mesons, Phys. Rev. D **74**, 074003 (2006).

- [4] U. G. Meißner, Loop effects in charmonium transitions, AIP Conf. Proc. **1322**, no.1, 266-274 (2010).
[5] F. K. Guo, C. Hanhart, G. Li, U. G. Meißner and Q. Zhao, Effect of charmed meson loops on charmonium transitions, Phys. Rev. D **83**, 034013 (2011).
[6] X. H. Liu and Q. Zhao, The Evasion of helicity selection rule in $\chi_{c1} \rightarrow VV$ and $\chi_{c2} \rightarrow VP$ via intermediate charmed meson loops, Phys. Rev. D **81**, 014017 (2010).

- [7] D. Y. Chen, J. He, X. Q. Li and X. Liu, Understanding the branching ratios of $\chi_{c1} \rightarrow \phi\phi, \omega\omega, \omega\phi$ observed at BES-III, Phys. Rev. D **81**, 074006 (2010).
- [8] F. K. Guo, C. Hanhart, G. Li, U. G. Meissner and Q. Zhao, Novel analysis of the decays $\psi' \rightarrow h_c\pi^0$ and $\eta'_c \rightarrow \chi_{c0}\pi^0$, Phys. Rev. D **82**, 034025 (2010).
- [9] X. H. Liu and Q. Zhao, Further study of the helicity selection rule evading mechanism in η_c, χ_{c0} and h_c decaying to baryon anti-baryon pairs, J. Phys. G **38**, 035007 (2011).
- [10] P. Colangelo, F. De Fazio and T. N. Pham, $B \rightarrow K^-\chi_{c0}$ decay from charmed meson rescattering, Phys. Lett. B **542**, 71 (2002).
- [11] D. Y. Chen, X. Liu and S. L. Zhu, Charged bottomonium-like states $Z_b(10610)$ and $Z_b(10650)$ and the $\Upsilon(5S) \rightarrow \Upsilon(2S)\pi^+\pi^-$ decay, Phys. Rev. D **84**, 074016 (2011).
- [12] C. Meng and K. T. Chao, Scalar resonance contributions to the dipion transition rates of $\Upsilon(4S, 5S)$ in the re-scattering model, Phys. Rev. D **77**, 074003 (2008).
- [13] C. Meng and K. T. Chao, Peak shifts due to $B^*\bar{B}^*$ rescattering in $\Upsilon(5S)$ dipion transitions, Phys. Rev. D **78**, 034022 (2008).
- [14] D. Y. Chen, J. He, X. Q. Li and X. Liu, Dipion invariant mass distribution of the anomalous $\Upsilon(1S)\pi^+\pi^-$ and $\Upsilon(2S)\pi^+\pi^-$ production near the peak of $\Upsilon(10860)$, Phys. Rev. D **84**, 074006 (2011).
- [15] D. Y. Chen, X. Liu and T. Matsuki, Explaining the anomalous $\Upsilon(5S) \rightarrow \chi_{bj}\omega$ decays through the hadronic loop effect, Phys. Rev. D **90**, 034019 (2014).
- [16] D. Y. Chen and X. Liu, $Z_b(10610)$ and $Z_b(10650)$ structures produced by the initial single pion emission in the $\Upsilon(5S)$ decays, Phys. Rev. D **84**, 094003 (2011).
- [17] C. Meng and K. T. Chao, $\Upsilon(4S, 5S)$ to $\Upsilon(1S)$ eta transitions in the rescattering model and the new BaBar measurement, Phys. Rev. D **78**, 074001 (2008).
- [18] X. Liu, B. Zhang and X. Q. Li, The Puzzle of excessive non- $D\bar{D}$ component of the inclusive $\psi(3770)$ decay and the long-distant contribution, Phys. Lett. B **675**, 441 (2009).
- [19] G. Li, X. h. Liu, Q. Wang and Q. Zhao, Further understanding of the non- $D\bar{D}$ decays of $\psi(3770)$, Phys. Rev. D **88**, 014010 (2013).
- [20] H. Y. Cheng, C. K. Chua and A. Soni, Final state interactions in hadronic B decays, Phys. Rev. D **71**, 014030 (2005).
- [21] Y. A. Simonov and A. I. Veselov, Bottomonium dipion transitions, Phys. Rev. D **79**, 034024 (2009).
- [22] D. Y. Chen, Y. B. Dong and X. Liu, Long-distant contribution and χ_{c1} radiative decays to light vector meson, Eur. Phys. J. C **70**, 177-182 (2010).
- [23] G. Li, Q. Zhao and B. S. Zou, Isospin violation in $\phi, J/\psi, \psi' \rightarrow \omega\pi^0$ via hadronic loops, Phys. Rev. D **77**, 014010 (2008).
- [24] G. Li and Q. Zhao, Revisit the radiative decays of J/ψ and $\psi' \rightarrow \gamma\eta_c(\gamma\eta'_c)$, Phys. Rev. D **84**, 074005 (2011).
- [25] Hong Chen, and Rong-Gang Ping, Polarization in $\chi_{cJ} \rightarrow \Lambda\bar{\Lambda}$ decays, Phys. Rev. D **102**, 016021 (2020).
- [26] M. G. Doncel, P. Mery, L. Michel, P. Minnaert, and K. C. Wali, Phys. Rev. **7**, 815 (1973).
- [27] R. Casalbuoni, A. Deandrea, N. Di Bartolomeo, R. Gatto, F. Feruglio and G. Nardulli, Phenomenology of heavy meson chiral Lagrangians, Phys. Rept. **281**, 145 (1997).
- [28] O. Kaymakcalan, S. Rajeev and J. Schechter, Nonabelian Anomaly and Vector Meson Decays, Phys. Rev. D **30**, 594 (1984).
- [29] Y. s. Oh, T. Song and S. H. Lee, J/ψ absorption by π and ρ mesons in meson exchange model with anomalous parity interactions, Phys. Rev. C **63**, 034901 (2001).
- [30] H. Y. Cheng, C. Y. Cheung, G. L. Lin, Y. C. Lin, T. M. Yan and H. L. Yu, Chiral Lagrangians for radiative decays of heavy hadrons, Phys. Rev. D **47**, 1030 (1993).
- [31] T. M. Yan, H. Y. Cheng, C. Y. Cheung, G. L. Lin, Y. C. Lin and H. L. Yu, Heavy Quark Symmetry And Chiral Dynamics, Phys. Rev. D **46**, 1148 (1992).
- [32] M. B. Wise, Chiral Perturbation Theory For Hadrons Containing A Heavy Quark, Phys. Rev. D **45**, R2188 (1992).
- [33] G. Burdman and J. F. Donoghue, Union of chiral and heavy quark symmetries, Phys. Lett. B **280**, 287 (1992).
- [34] A. F. Falk and M. E. Luke, Strong decays of excited heavy mesons in chiral perturbation theory, Phys. Lett. B **292**, 119 (1992).
- [35] P. A. Zyla *et al.* [Particle Data Group], PTEP **2020**, no.8, 083C01 (2020).
- [36] M. Benayoun, L. DelBuono, S. Eidelman, V. N. Ivanchenko and H. B. O'Connell, Radiative decays, nonet symmetry and SU(3) breaking, Phys. Rev. D **59**, 114027 (1999).
- [37] A. Kucukarslan and U. G. Meißner, Omega-phi mixing in chiral perturbation theory, Mod. Phys. Lett. A **21**, 1423-1430 (2006).
- [38] S. I. Dolinsky, V. P. Druzhinin, M. S. Dubrovin, V. B. Golubev, V. N. Ivanchenko, E. V. Pakhtusova, A. N. Peryshkin, S. I. Serebnyakov, Y. M. Shatunov and V. A. Sidorov, *et al.* Summary of experiments with the neutral detector at the e^+e^- storage ring VEPP-2M, Phys. Rept. **202**, 99-170 (1991).
- [39] H. Chen and R. G. Ping, Polarization in $\chi_{cJ} \rightarrow \phi\phi$ decays, Phys. Rev. D **88**, no.3, 034025 (2013).
- [40] M. Ablikim *et al.* [BESIII], Observation of the helicity-selection-rule suppressed decay of the χ_{c2} charmonium state, Phys. Rev. D **96**, no.11, 111102 (2017).
- [41] M. Ablikim *et al.* [BESIII], Future Physics Programme of BE-III, Chin. Phys. C **44**, no.4, 040001 (2020).